Journal of Power Sources 185 (2008) 1040–1048

Contents lists available at ScienceDirect

Journal of Power Sources

journal homepage: www.elsevier.com/locate/jpowsour

# Effects of operating temperatures on performance and pressure drops for a 256 $cm^2$ proton exchange membrane fuel cell: An experimental study

Wei-Mon Yan[a], Xiao-Dong Wang[b,*], Sen-Sin Mei[a], Xiao-Feng Peng[c], Yi-Fan Guo[a], Ay Su[d]

[a] Department of Mechatronic Engineering, Huafan University, Shih-Ting 22305, Taiwan
[b] Department of Thermal Engineering, School of Mechanical Engineering, University of Science and Technology Beijing, Beijing 100083, China
[c] Lab of Phase Change & Interfacial Transport Phenomena, Tsinghua University, Beijing 100084, China
[d] Department of Mechanical Engineering & Fuel Cell Center, Yuan Ze University, Taoyuan, 320, Taiwan

ARTICLE INFO

*Article history:*
Received 22 July 2008
Accepted 20 August 2008
Available online 27 August 2008

*Keywords:*
Cell temperature
Humidification temperature
Serpentine flow field
Performance
Pressure drop

ABSTRACT

Cell performance and pressure drop were experimentally investigated for two commercial size 16 cm × 16 cm serpentine flow field proton exchange membrane fuel cells with Core 5621 and Core 57 membrane electrode assemblies at various cell temperatures and humidification temperatures. At cell temperature lower than the humidification temperature, the cell performance improved as the cell temperature increased, while reversely at cell temperature higher than the humidification temperature. At a specified cell temperature, increasing the cathode and/or anode humidification temperature improved the cell performance, and their effects weakened as cell temperature decreased. The effects of the cell and the humidification temperature on the pressure drops were closely related to the reactant feed mode. For the constant stoichiometric flow rate mode, both cathode and anode pressure drops increased as humidification temperature and average current density increased. For the constant mass flow rate mode, both cathode and anode pressure drops increased as humidification temperature increased, while anode pressure drops decreased and cathode pressure drops increased as average current density increased. The optimal cell performance occurred at cell temperature of 65 °C and humidification temperature of 70 °C. The effects of these operating parameters on the cell performance and pressure drop were analyzed based on the catalytic activity, membrane hydration, and cathode flooding.



## 1. Introduction

Fuel cells are electrochemical devices that can realize direct conversion of the chemical energy in the reactants to electrical energy with high efficiency and high environment compatibility. A proton exchange membrane fuel cell (PEMFC) operates at significantly lower temperatures than other types of fuel cells, and was received much attention in the last decade due to its many promising applications in portable power sources, automobile power systems, and stationary power plants [1–4].

The flow field design in the bipolar plates is one of the most important issues in a PEMFC. An appropriate flow field design can improve the reactant transport and the efficiency of the thermal and water management. So far, there are different flow field configurations, including parallel, serpentine, interdigitated, and many other combined versions, developed by different researchers. Many efforts were devoted to the optimal flow field design for improving cell performance [5–22]. The cell performance is also dependent on operating conditions such as temperature, pressure, and humidification of the reactants [23–35], closely related to water and heat management in a PEMFC. Normally a proton exchange membrane must be well hydrated to maintain high proton conductivity. On the other hand, cathode electrochemical reactions produce water and water is also transported from the anode to the cathode by electro-osmosis. Obviously, if excessive liquid water accumulates in the pores of the cathode porous gas diffusion layer and catalyst layer, the oxygen transport resistance increases and the cell performance is reduced. Control of a cell temperature is another important parameter. High cell temperature increases catalytic activity and decrease mass transport resistance. Also, a very high cell temperature may cause the membrane dehydration or membrane dry-out, even though it significantly increases proton transport resistance. Thus, a proper combination of the cell temperature and humidification temperature is important to ensure high cell performance. In order to improve cell performances, it is essential to understand these parameters on cell performance. In the recent years, fuel cell companies and research institutes may have carried out various systematic experimental studies in this area for different specific purposes, but most of the data would be proprietary in nature and very limited data are available in the open literature. Yet system-

* Corresponding author. Tel.: +86 10 62321277; fax: +86 10 81765088.
*E-mail address:* wangxd99@gmail.com (X.-D. Wang).

0378-7753/$ – see front matter © 2008 Elsevier B.V. All rights reserved.
doi:10.1016/j.jpowsour.2008.08.053

**Nomenclature**

| | |
|---|---|
| $I$ | average current density (A m$^{-2}$) |
| $P$ | pressure (Pa) |
| $T_{cell}$ | cell temperature |
| $T_{in}$ | humidification temperature (K) |
| $T_{in,a}$ | anode humidification temperature (K) |
| $T_{in,c}$ | cathode humidification temperature (K) |
| $V_{cell}$ | operating voltage (V) |

atic experimental data are very valuable for fuel cell developers to optimize their fuel cell operating conditions according to their specific fuel cell designs and operation requirements, and to accelerate their fuel cell design and optimization. Such data are also essential for fuel cell model developers to validate and improve their models.

Wang et al. [23,24] experimentally investigated the effect of operating parameters on the performance of 7.2 cm × 7.2 cm PEMFC with interdigitated flow field using pure hydrogen on the anode side and air on the cathode side. Nguyen and Knobbe [25] employed a new exhaust system to study the effects of the interdigitated flow field on the reactant consumption and liquid water removal. The continuous exhausting system could augment the efficiency of removing liquid water accumulated in the gas diffusion layer to improve the cell performance. Amirinejad et al. [26] experimentally investigated the performance of a 5 cm$^2$ PEMFC under various operating conditions using dry and humidified hydrogen and oxygen as reactants. The optimum conditions were at higher pressure and elevated temperature with the humidified reactants. Furthermore, a pressurized cathode side was better than a pressurized anode side. Yan et al. [27,28] experimentally investigated the effect of operating conditions including cathode inlet mass flow rate, cathode inlet humidification temperature, cell temperature on the performance of 14.1 cm × 14.1 cm PEMFCs with the interdigitated and conventional flow fields. The cell performance was enhanced with an increase in the cathode inlet flow rate, cathode humidification temperature and cell temperature and the cells with the flow area ratio of 40.23 or 50.75% have better performance than the cell with the flow area ratio of 66.75%. Yan et al. [29] measured the optimal cathode reactant flow rates of PEMFCs with different flow field designs, including the parallel flow field, Z-type flow field, serpentine flow field, parallel flow field with baffle and Z-type flow field with baffle. The interdigitated flow field designs were found better than the conventional flow field, because the baffle forced the reactants through the gas diffusion layer and the catalyst layer, and the parallel flow field with baffle provided the best cell performance among the five flow field designs. Yan et al. [30] experimentally investigated the steady-state performance and transient response of 5 cm$^2$ PEMFC under a variety of loading cycles and operating conditions. A decrease in the cathode humidity resulted in a detrimental effect on fuel cell steady state and dynamic performance. The cell performance was improved with increasing temperature from 65 to 75 °C and as the operating pressure was increased from 1 to 4 atm. Xu et al. [31] experimentally investigated the polarization losses of 5 cm$^2$ PEMFC with serpentine flow field at 120 °C and reduced relative humidity. As the cell temperature increases and/or relative humidity decreases, the polarization losses of the cell significantly increase, therefore, design of electrodes is extremely important for high temperature PEMFCs. Sun et al. [32] experimentally studied the effect of different anode and cathode humidification temperatures on local current densities of 4.0 cm × 4.0 cm PEMFC with a co-flow serpentine flow field. Both air and the hydrogen needed to be humidified to ensure optimal cell performance, and too high or too low humidification temperature could cause severe non-uniform distribution of local current density. Hsieh and Chu [33] experimentally examined the effects of channel and rib widths with an aspect ratio of 0.67 of rectangular cross-sections flow field plates on cell performance of 5 cm$^2$ PEMFCs. Their results showed that an optimum channel-to-rib width ratio in the range of the present study of 0.5–2 was found to be 0.67 as far as the net power gain (power gain/power consumption) was concerned. However, if only polarization curves were considered, the above-stated value would become a little bit bigger, and it was found to be one. Zhang et al. [34] experimentally investigated the cell performance of 4.4 cm$^2$ PEMFC with serpentine flow field in the temperature range of 23–120 °C, with dry reactants. Their results showed that the limited proton transfer process to the Pt catalysts, mainly in the inonomer within the membrane electrode assembly (MEA) could be responsible for the performance drop. It was demonstrated that operating a fuel cell using a commercially available membrane (Nafion® 112) is feasible under certain conditions without external humidification. However, the cell performance without external humidification decreased with increasing operation temperature and reactant flow rate and decreasing operation pressure. Kadjo et al. [35] experimentally investigated the effect of the cell temperature, humidification temperature, and reactant flow rates and pressures on the performance of a 25 cm$^2$ PEMFC. They tested two different homemade MEAs under optimal operating conditions. Their results showed that the decrease of the platinum loading in the cathode from 0.35 to 0.1 mg cm$^{-2}$ affects the oxygen reduction kinetics and the cell ohmic resistance, and hence the cell performance.

In most available experimental studies, active area of the PEMFC usually is less than 25 cm$^2$, there are a few experimental studies dealing with large size PEMFC [27–29]. In this work, the cell performance and the pressure drops of the commercial size 256 cm$^2$ PEMFCs with serpentine flow field was experimentally investigated at various cell temperatures and cathode/anode humidification temperatures for a single PEMFC. An attempt was made to provide systematic experimental data that may be valuable for the fuel cell developers and better understanding the fundamentals.

## 2. Experiment

### 2.1. Experimental setup

In this work, the Advanced Screener Test Station Hydrogenics FCATS S-2000 fuel cell testing system was employed to control the cell operation and measure voltage–current (polarization) curves. Fig. 1 shows a schematic of the experimental apparatus, which consists of a gas supply system, a flow rate control system, a temperature control system, a humidifier system, an electric load system, a data acquisition system and a test section. The gas supply system supplied hydrogen, oxygen or air as the anode and cathode reactants to the fuel cell. Nitrogen gas was supplied to purge the residual gas inside the cell before and after each test. The flow rate control system controlled the gas inlet flow rate following stoichiometric or constant mode. The temperature control system, which included a heating rod, type-T thermocouples and Omega CN760000 PID temperature controller, was used to control the cell temperature. The humidification system forced the reactants through humidification bottles and regulated the temperature of the humidified reactants. The electric load system enables the maximum power output of 2000 W and the maximum current of 400 A.

Before collecting cell performance data, the unit cell was preconditioned by operating them potentiostatically at 0.6 V for a minimum of 24 h. For polarization measurement, the cell operated in the potentialstatic (controlled voltage) mode. Initially, the voltage was set to be 1.0 V and then decreased by a 0.05 V for each

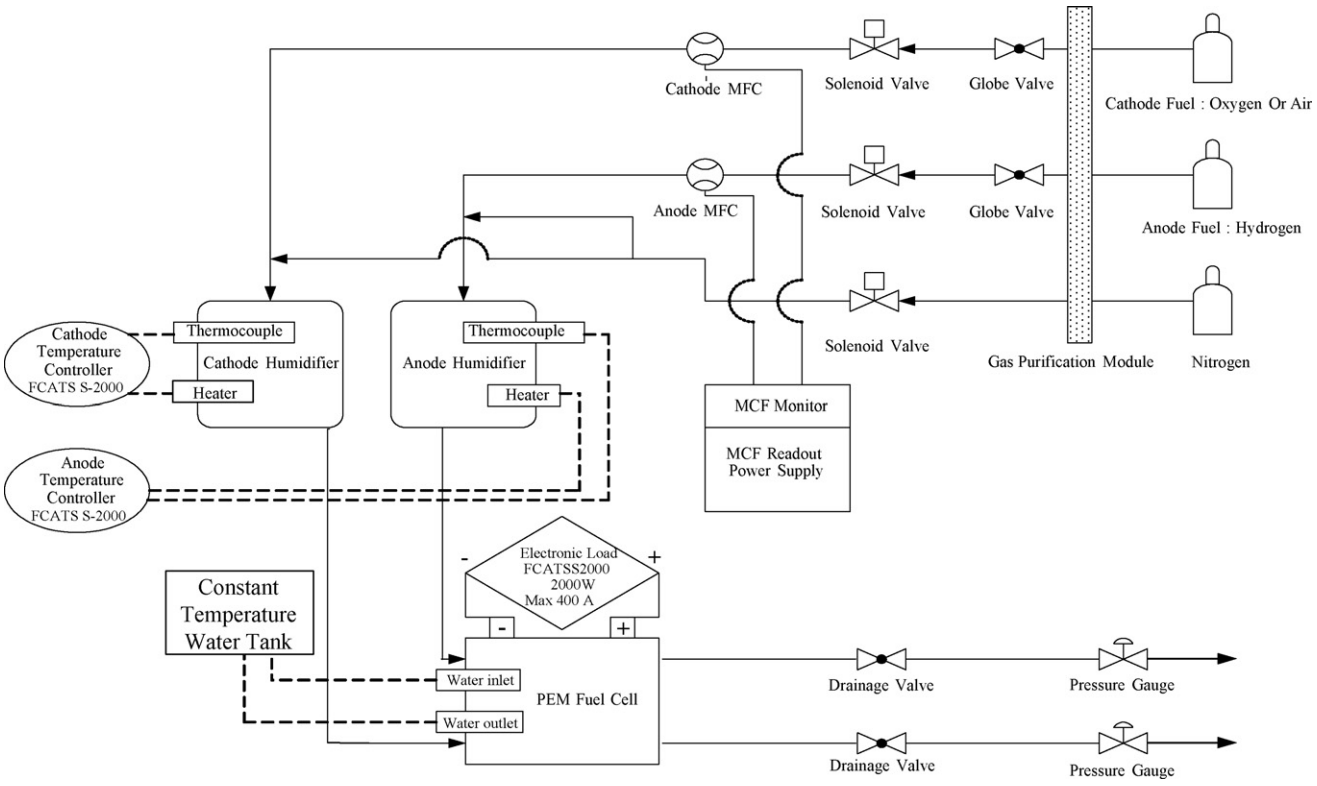


**Fig. 1.** Schematic of experimental setup.

measurement. The output current was the average over 30 s after the initial transient.

### 2.2. Materials and size of fuel cell

A PEM fuel cell usually consists of seven layers, i.e., cathode flow field plate, cathode gas diffusion layer, cathode catalyst layer, proton exchange membrane, anode catalyst layer, anode gas diffusion layer and anode flow field plate. In the present experiment, a GORE-TEX® PRIMRA5621 MEA with 16 cm × 16 cm active surface area was used, which consisted of a proton exchange membrane of 35 μm thickness, an anode catalyst layer with 0.45 mg cm$^{-2}$ Pt content, a cathode catalyst layer with 0.6 mg cm$^{-2}$ Pt and Ru contents, providing a catalyst effective reaction area of 16 cm × 16 cm. For comparison sake, a GORE-TEX® PRIMRA57 MEA was also used which consisted of a proton exchange membrane of 18 μm thickness, an anode catalyst layer with 0.2 mg cm$^{-2}$ Pt content, a cathode catalyst layer with 0.4 mg cm$^{-2}$ Pt and Ru contents. The material of the gas diffusion layer was GDL 10BC carbon paper (SGL company), which had a size of 16 cm × 16 cm and a thickness of 366 μm. The material of the end plate used in this work was aluminum alloy 7075 with a cross-section of 22 cm × 22 cm and a thickness of 4 cm. The collector plate was made of highly conductive copper and gold plated on the surface to increase its surface conductivity and reduce contact resistance to bipolar plate. The collector plate had a size of 16 cm × 16 cm and thickness of 0.2 cm. The material for the gasket was Teflon, and its size was 20.5 cm × 20.5 cm and its thickness was 0.03 cm. The bipolar plate in experiments was a pure graphite plate (SCHUNK company), which had a size of 20.5 cm × 20.5 cm, a thickness of 0.3 cm. In the present experiments, the PEMFC with two identical serpentine flow field (one is anode and another is cathode) was investigated experimentally. Fig. 2 shows the schematic of the flow field, which includes 16 serpentine loops and has a size of 16 cm × 16 cm.

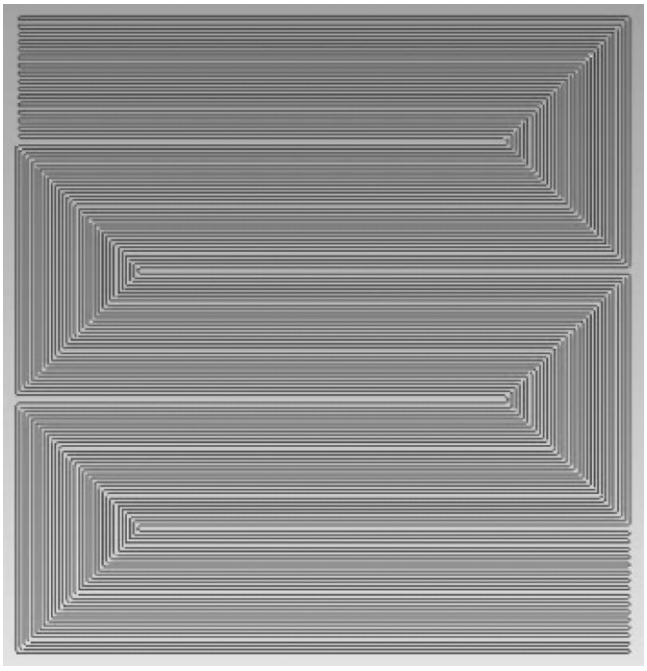

**Fig. 2.** Serpentine flow field design used in the present experiments.

## 3. Results and discussion

### 3.1. Effect of cell temperature

In the experiments, the cathode and anode reactants were fed with the constant stoichiometric flow rates of 4.0/1.8 on cathode/anode sides; the reactant inlet humidification temperature on

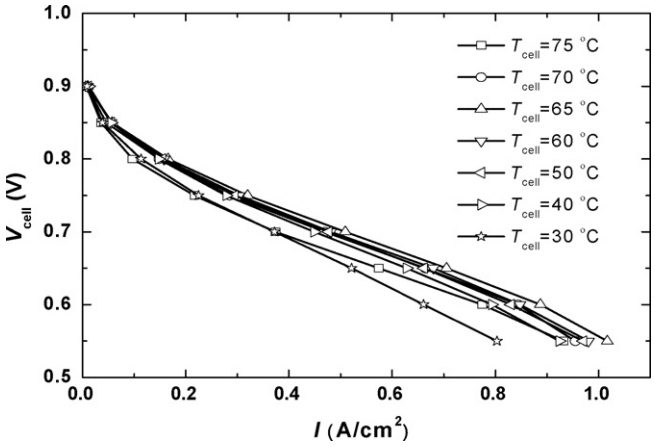


**Fig. 3.** Effect of cell temperature on the cell performance at humidification temperature of 70 °C.

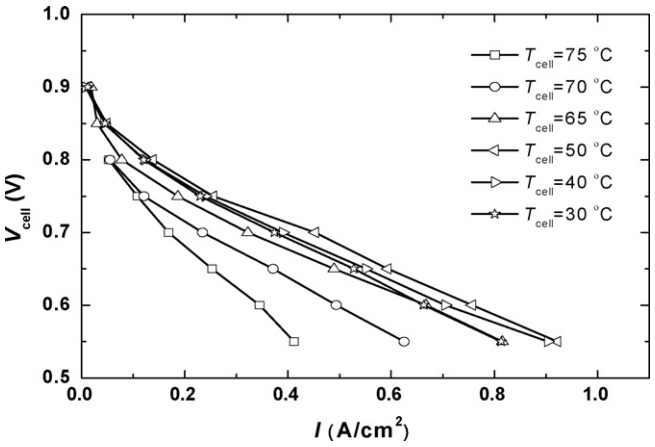


**Fig. 5.** Effect of cell temperature on the cell performance at humidification temperature of 50 °C.

cathode and anode sides were the same and were set to be 30, 50, 60, and 70 °C; the cell temperature were set to be 30, 40, 50, 60, 70, and 75 °C.

Fig. 3 shows a set of polarization curves at various cell temperatures and a specified humidification temperature of 70 °C. As the cell temperature increased from 30 to 65 °C, the average current density increased and cell performance was improved, because increasing cell temperature not only enhanced catalytic activity but also accelerated evaporation of liquid water in the cell. If excessive liquid water accumulated in the pores of the gas diffusion layer and catalyst layer, the oxygen transport resistance would increase and cell performance would be reduced. However, as the cell temperature was higher than the humidification temperature, the cell performance became worse as increasing cell temperature. When the cell temperature was higher than the humidification temperature, the membrane hydration would not be maintained due to extreme evaporation of liquid water in the cell, which significantly increased ohmic impedance of membrane.

Figs. 4–6 show the polarization curves for the various cell temperatures at the humidification temperatures of 60, 50, and 30 °C, respectively. Very clearly, the cell performance was improved with increasing cell temperature at cell temperature lower than the humidification temperature; however, it became worse at cell temperature higher than the humidification temperature. Increasing cell temperature enhanced catalytic activity and decreased cathode liquid flooding, improving the cell performance. On the other hand, increasing cell temperature could also induce membrane dry-out, which reduced the cell performance. At the cell temperature lower than the humidification temperature, more water vapor introduced from the flow channel inlet and produced by cathode electrochemical reaction could condense in the cell, which ensured membrane hydration. However, too low cell temperature resulted in excessive liquid water formed in the cell, which increased cathode flooding. Therefore, the cell performance was improved with increasing cell temperature. At the cell temperature higher than the humidification temperature, the evaporation rates of liquid water in the cell were significantly accelerated, and resulted in the membrane dry-out and the increase in the proton transport resistance. In addition, Figs. 4–6 show that for a specified humidification temperature the cell performance at the cell temperature of 30 °C was better than at 75 °C, indicating the membrane dry-out produced by high cell temperature had more important effect on the cell performance than decreasing catalytic activity and increasing cathode flooding produced by low cell temperature.

### 3.2. Effect of humidification temperature

Fig. 7 shows the effect of the cell temperature on the average current density at various humidification temperatures and operating voltage of 0.7 V. For the cell temperature of 40–75 °C, at the same cell temperature the cell performance became worse with decreasing humidification temperature, and the optimal cell performance

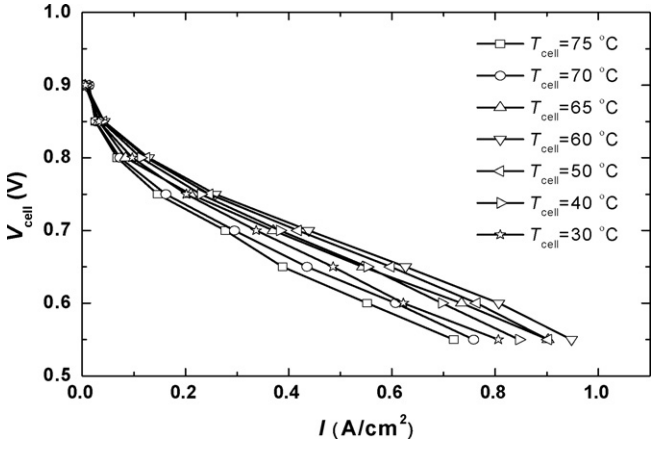


**Fig. 4.** Effect of cell temperature on the cell performance at humidification temperature of 60 °C.

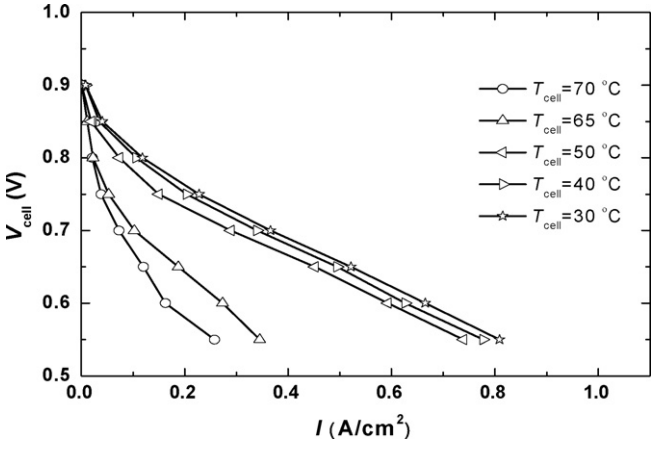


**Fig. 6.** Effect of cell temperature on the cell performance at humidification temperature of 30 °C.

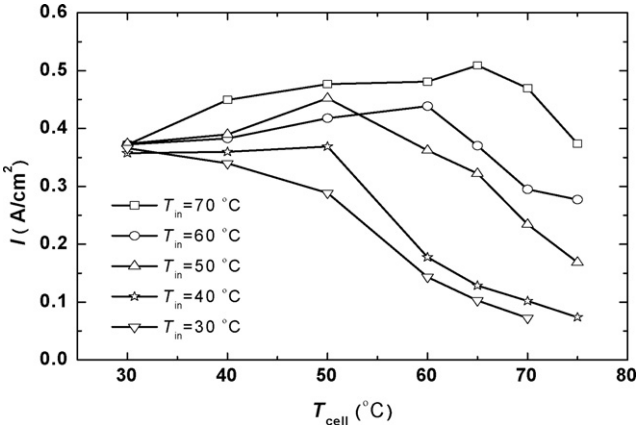


**Fig. 7.** Effect of cell temperature and humidification temperature on current density at operating voltage of 0.7 V.

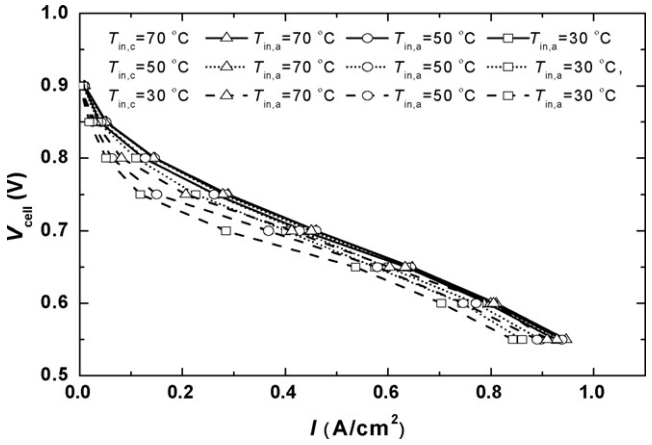


**Fig. 9.** Effect of cathode and anode humidification temperature on cell performance at cell temperature of 50 °C.

occurred at the humidification temperature of 70 °C. Normally increasing humidification temperature increases the amount of water vapor in the inlet reactants, which provides more water for the membrane at the same cell temperature and improves the membrane hydration. In addition, Fig. 7 also indicates that as the cell temperature decreased, the effect of the humidification temperature on the cell performance gradually weakened. Especially, at the cell temperature of 30 °C the humidification temperature almost did not affect the cell performance, indicating at too lower cell temperature, even though for the humidification temperature of 30 °C, the membrane hydration also could be ensured due to high condensation rates of water vapor, so the cell performance was not dependent on the humidification temperature.

### 3.3. Effect of cathode and anode humidification temperature

To analyze cathode and anode humidification temperatures on cell performance at various cell temperatures, the cell temperature was set to be 30, 50, and 65 °C, and the cathode and anode humidification temperatures were set to be 30, 50, and 70 °C. Figs. 8–10 show the polarization curves for various combinations of the cathode and anode humidification temperatures with the specified cell temperatures of 65, 50, and 30 °C. Fig. 8 indicates that with a specified cell temperature of 65 °C, at the same cathode humidification temperature, the cell performance increased with increasing anode humidification temperature, so the optimal cell performance occurred for the anode humidification temperature of 70 °C. Because increasing anode humidification temperature increased the amount of water vapor in the anode inlet reactants, which provided more water for the membrane on anode side at the same cell temperature. Figs. 9 and 10 indicate that at the specified cell temperatures of 50 and 30 °C, at the same cathode humidification temperature the cell performance also increased with increasing anode humidification temperature. However, as the cell temperature decreased, the effect of the anode humidification temperature on the cell performance gradually weakened. This is because decreasing cell temperature reduced evaporation rates of water vapor in the cell, which reduced liquid water removal from the cell and ensured the membrane hydration, so the effect of the anode humidification temperature on the cell performance weakened.

The effect of the cathode humidification temperature on the cell performance was similar to the anode humidification temperature. Though the cathode electrochemical reactions produced water, the air inlet mass flow rate on the cathode side was far higher than the anode inlet mass flow rate, so liquid water on the cathode side produced by electrochemical reactions should be rapidly removed out of the cell, which caused the membrane on the cathode side to dry out, therefore, the cathode humidification of reactant was also needed. Fig. 11 shows the polarization curves for various cell temperatures and anode humidification

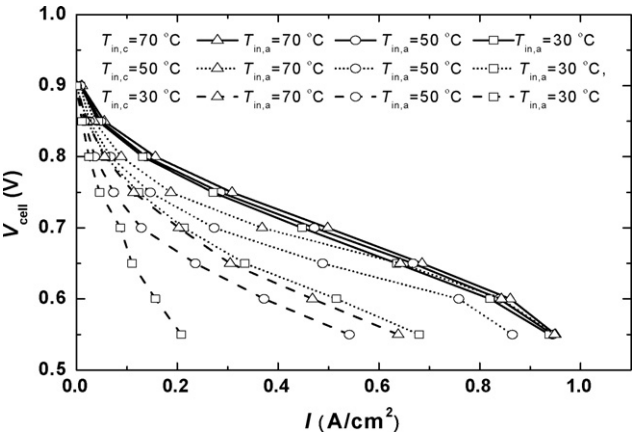


**Fig. 8.** Effect of cathode and anode humidification temperature on cell performance at cell temperature of 65 °C.

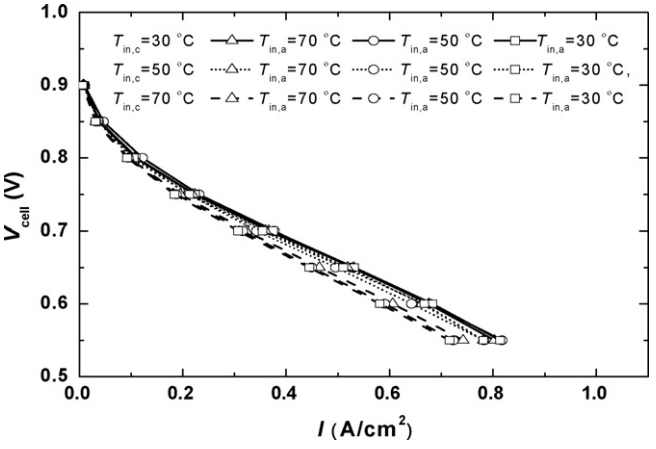


**Fig. 10.** Effect of cathode and anode humidification temperature on cell performance at cell temperature of 30 °C.

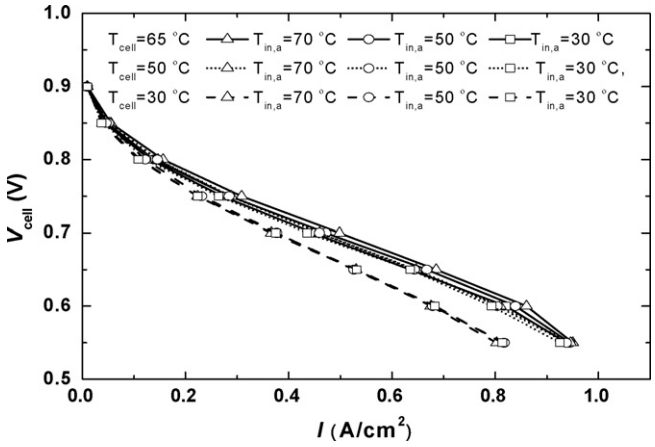


**Fig. 11.** Effect of cell temperature and anode humidification temperature on cell performance at cathode humidification temperature of 70 °C.

temperatures with a specified cathode humidification temperature of 70 °C. Fig. 11 indicates that at the same cell temperature, with a sufficiently high cathode humidification temperature the anode humidification temperature had a small effect on the cell performance. At a higher cathode humidification temperature more water vapor was introduced from cathode flow channel inlet to the cathode side of the cell, in addition, the cathode electrochemical reactions also produced water; high water concentration on cathode side enhanced back-diffusion of liquid water from the cathode to the anode, which increased the hydration of the membrane on the anode side and weakened the effect of the anode humidification temperature on the cell performance. Figs. 8–10 also show that the cell performance improved more significantly with increasing cathode humidification temperature than with increasing anode humidification temperature, indicating that the cathode humidification temperature had stronger effect on the cell performance than the anode humidification temperature.

Comparison of Figs. 8–10 shows that at the cell temperature of 65 °C, the cell performance significantly increased with increasing cathode and anode humidification temperatures because the higher cell temperature increased the evaporation rates of water vapor in the cell, so maintaining the membrane hydration needed higher cathode and/or anode humidification temperatures. At the higher cathode and anode humidification temperatures, the cell performance at the cell temperature of 50 °C was worse than that at the cell temperature of 65 °C because when membrane had enough water, increasing cell temperature enhanced the catalytic activity and reduced the cathode flooding, so the cell performance improved. However, at the lower cathode and anode humidification temperature, the cell performance at the cell temperature of 50 °C was better than that at the cell temperature of 65 °C, and this was especially apparent at the cathode and anode humidification temperature of 30 °C. Though the higher cell temperature enhanced the catalytic activity, the higher cell temperature and the lower humidification temperature caused the membrane to dry out. Under this operating condition, the membrane hydration was the more important factor affecting the cell performance than the catalytic activity, so the cell performance decreased with increasing cell temperature. At the cell temperature of 30 °C, the cathode and anode humidification temperatures had less effect on the cell performance, indicating at a too low cell temperature, membrane hydration was not a key factor affecting the cell performance because high condensation rates of water vapor in the cell provided the membrane for enough water.

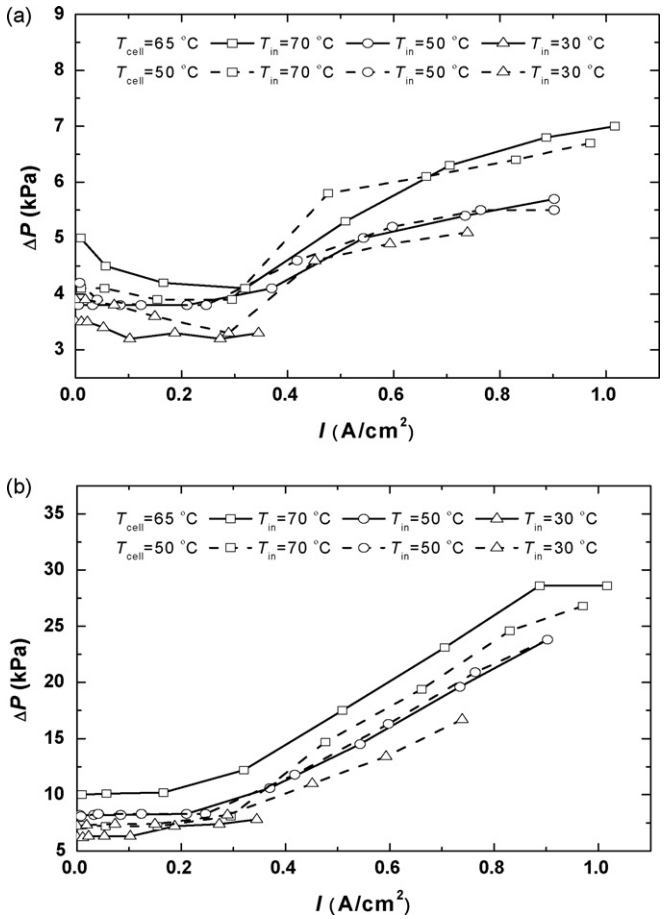


**Fig. 12.** Effect of cell temperature and humidification temperature on cell pressure drops for the constant stoichiometric flow rates: (a) anode pressure drops and (b) cathode pressure drops.

### *3.4. Pressure drops for various cell temperatures and humidification temperatures*

The operating condition influences not only the cell performance but also the pressure drop in the fuel cell. Larger pressure drops in the fuel cell mean that more power is needed to pump the reactants. Thus, the pressure drop is also a significant issue in addition to the polarization curve. This section discusses the effect of the cell temperature and the humidification temperature on the pressure drop. The reactants were fed using two modes in the present experiments, i.e., constant mass flow rates and constant stoichiometric flow rates.

Fig. 12(a) and (b) show the anode and cathode pressure drops for various cell temperatures and various humidification temperatures with the constant anode/cathode stoichiometric flow rates of 1.4/4. Fig. 12(a) and (b) indicate that at lower current densities, the pressure drops were lower because the electrochemical reaction rates were slower with a lower reactant inlet mass flow rates and a small amount of liquid water was produced. However, at higher current densities, the electrochemical reaction rates gradually increased with more reactant consumptions, which increased the reactant inlet mass flow rates and produced more liquid water, so the pressure drops increased as the current density increased. Fig. 12(a) and (b) also indicate that at the same cell temperature, as the cathode and/or anode humidification temperatures increased, the pressure drops increased. Higher humidification temperature increased the amount of water vapor in the reactants, therefore, at

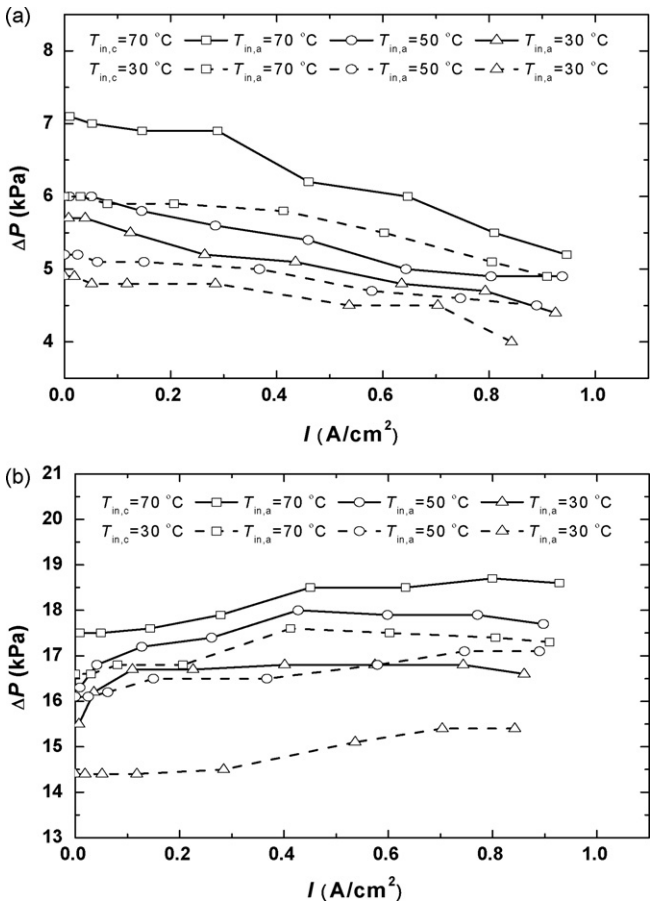


**Fig. 13.** Effect of cell temperature and humidification temperature on cell pressure drops for the constant mass flow rates: (a) anode pressure drops and (b) cathode pressure drops.

the same cell temperature more water vapor should be condensed to liquid water, which decreased the effective cross-sectional area of the flow channel, so the pressure drops increased with increasing humidification temperature. In addition, Sections 3.2 and 3.3 indicate that at the same cell temperature, the cell performance improved as the humidification temperature increased; hence the reactant inlet mass flow rates increased, which also increased the pressure drops. Comparison of Fig. 12(a) and (b) indicates that the pressure drops on the cathode side was far higher than that on the anode side because the cathode stoichiometric flow rate is higher than the anode stoichiometric flow rate, and also because cathode electrochemical reaction produced water.

Fig. 13(a) and (b) show the anode and cathode pressure drops for various cell temperatures and various humidification temperatures with the constant anode/cathode mass flow rates of 2000 $cm^3\ min^{-1}$/15,000 $cm^3\ min^{-1}$. Fig. 13(a) shows that at the same cell temperature and the same cathode humidification temperature, as the anode humidification temperature increased the anode pressure drops increased. Higher anode humidification temperature increased the content of water vapor in the anode inlet reactants, thus, at the same cell temperature more water vapor was condensed to liquid water, which decreased the effective cross-sectional area of the flow channel, so the pressure drops increased. Similarly, at the same cell temperature and the same anode humidification temperature, as the cathode humidification temperature increased the anode pressure drops increased. This is because as the cathode humidification temperature increased the more liquid water was transported from the cathode to the anode by back-diffusion, which increased anode pressure drops. It was different from the constant stoichiometric flow rates, for the constant mass flow rates, the anode pressure drops decreased as the current density increased because higher current density meant the stronger electrochemical reaction rates with more hydrogen consumption, so the anode outlet mass flow rates decreased with increasing current density, which decreased the anode pressure drops. Fig. 13(b) shows that at the same cell temperature and the same cathode humidification temperature, as the anode humidification temperature increased the cathode pressure drops increased. Because as the anode humidification temperature increased the cell performance improved and average current densities increased, which caused more liquid water to be transported from the anode to the cathode by electro-osmosis and which also caused more liquid water to be produced at the cathode by the electrochemical reactions. At the same cell temperature and the same anode humidification temperature, as the cathode humidification temperature increased the cathode pressure drops increased. Because as the cathode humidification temperature increased the cell performance improved, thus, more liquid water was produced at the cathode. Opposite to the anode pressure drops, the cathode pressure drops slightly increased as the average current density increased. As the average current density increased, more cathode reactant was consumed and cathode outlet mass flow rate was reduced, which decreased the cathode pressure drops. On the other hand, as the average current density increased, the cathode electrochemical reactions produced more liquid water, which increased the cathode pressure drops. Above result showed that liquid water formation had larger effect on the cathode pressure drops.

### 3.5. Effect of reactant inlet mass flow rates

Fig. 14 shows the effect of the reactant inlet mass flow rates on the cell performance at various cell temperatures with a specified cathode/anode humidification temperature of 70 °C. Fig. 14 shows that as the cathode/anode mass flow rates increased, the cell performance improved and the optimal cell performance all occurred at the cell temperature of 65 °C for various cathode/anode mass flow rates, which again confirmed the conclusion in Section 3.1. With a cathode mass flow rate of 6000 $cm^3\ min^{-1}$ and an anode mass flow rate of 800 $cm^3\ min^{-1}$, there were serious concentration polarizations and the cell had the almost same performance for all the cell temperatures at the operating voltage lower than 0.7 V, which indicated that hydrogen was almost completely consumed, hence cell temperature no longer affected the cell performance. With a cathode mass flow rate of 9000 $cm^3\ min^{-1}$ and an anode mass flow rate of 1500 $cm^3\ min^{-1}$, the cell performance increased and there were also concentration polarizations at low operating voltages; however, the concentration polarizations occurred at a lower operating voltage of 0.6 V. As the cathode/anode mass flow rates continued to increase, the cell performance continuously improved while with a weaker effect at higher reactant mass flow rates, especially this was true at the optimal cell performance of 65 °C. Therefore, in the present study, the optimal mass flow rates were 12,000 $cm^3\ min^{-1}$ on the cathode side and 2000 $cm^3\ min^{-1}$ on the anode side. Moreover, the polarization curves intersected for cell temperatures of 30 and 80 °C. At higher operating voltages, the 80 °C cell temperature resulted in serious membrane dehydration so the cell performance at 80 °C was lower than at 30 °C. However, at lower operating voltages, the strong electrochemical reaction produced more liquid water which maintained the membrane hydration very well. At cell temperature of 30 °C, the excessive liquid water was produced by condensation due to lower cell temperature, so that the cell performance was better at 80 °C.

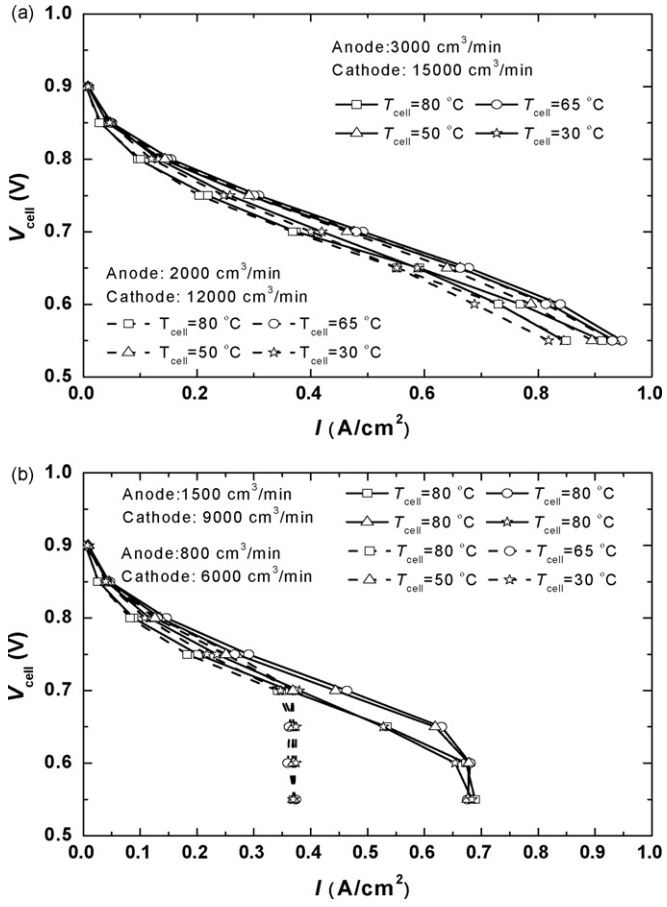


**Fig. 14.** Effect of reactant inlet mass flow rates on the cell performance at various cell temperatures with a specified anode/cathode humidification temperature of 70 °C.

### 3.6. Effect of MEAs

Fig. 15 shows the polarization curves at the various cell temperatures with a specified cathode/anode humidification temperature of 50 °C for Core 5621 and Core 57. Fig. 15 again shows that for both MEAs when the cell temperature was lower than the humidification temperature, the cell performance increased as the cell temperature increased, while reversely at cell temperature higher than the humidification temperature. Fig. 15 also shows that when the cell temperature ranged from 30 to 50 °C, the cell performance of Core 57 was better than that of Core 5621, while the cell temperature increases to 75 °C, the cell performance of Core 57 was far better than that of Core 5621. The above results indicated that at specified cell temperature and humidification temperature, the Core 57 had a better cell performance than Core 5621 because the thinner membrane Core 57 was easily hydrated than thicker membrane Core 5621. Especially, as the cell temperature increased to 75 °C the evaporation rates of liquid water significantly increased, which enhanced the liquid water removal. For the thicker membrane Core 5621, the water amount in the membrane was far not enough to efficiently transport the proton compared with membrane Core 57, which resulted in very high membrane ohmic impedance and a very low cell performance.

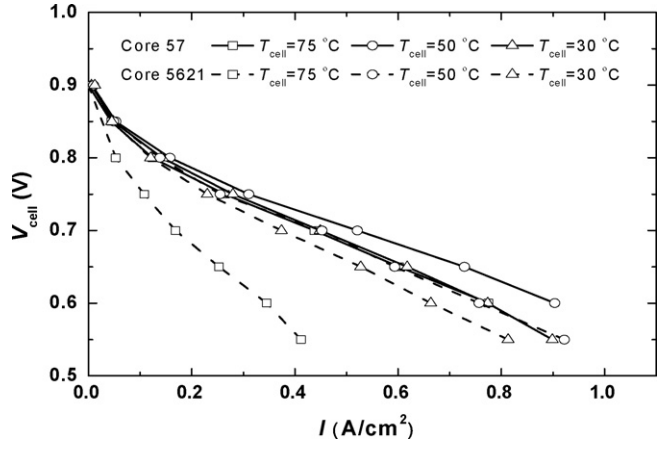


**Fig. 15.** Polarization curves of PEMFCs with Core 5621 and Core 57 MEAs at various cell temperatures with a specified anode/cathode humidification temperature of 50 °C.

## 4. Conclusions

This paper experimentally investigated the effect of the cell temperature and the cathode/anode humidification temperatures on the cell performance and the pressure drops for 16 cm × 16 cm PEMFCs with the serpentine flow field and two different MEAs Core 5621 and Core 57. Based on the above experimental results, the following conclusions can be drawn:

1. For the cell temperature lower than the humidification temperature, the cell performance improved as the cell temperature increased, while reversely at cell temperature higher than the humidification temperature. Therefore, optimal cell performance was dependent on a proper combination of the cell temperature and humidification temperature.
2. At the same cell temperature, as the humidification temperature increased the cell performance improved. As the cell temperature decreased the effect of the humidification temperature on the cell performance weakened. Especially, when cell temperature decreased to 30 °C, the humidification temperature almost did not affect the cell performance.
3. At the same cell temperature and the same anode humidification temperature, as cathode humidification temperature increased the cell performance improved. Similarly, at the same cell temperature and the same cathode humidification temperature, as the anode humidification increased the cell performance improved. The cathode humidification temperature had more significant effect on the cell performance than the anode humidification temperature at least in our test conditions.
4. The effects of the cell temperature and the humidification temperature on the pressure drops were closely related to the reactant feed mode. For the constant stoichiometric flow rates, the cathode and anode pressure drops increased as the humidification temperature and the average current density increased. For the constant mass flow rates, the cathode and anode pressure drops increased as the humidification temperature increased, the anode pressure drops decreased as the average current density increased, cathode pressure drops increased as the average current density increased. The optimal cell performance occurred for the cell temperature of 65 °C and the humidification temperature of 70 °C.

## Acknowledgements

This study was supported by the National Science Council of Taiwan (Grant No. NSC 94-2212-E-211-004) and the National Natural Science Foundation of China (Grant No. 50636030 and No. 50876009).

## References


[1] J. Larmine, A. Dicks, Fuel Cell Systems Explained, 2nd ed., Wiley, Chichester, West Sussex, 2003.
[2] H. Yang, T.S. Zhao, Q. Ye, J. Power Sources 139 (2005) 79.
[3] X.G. Li, I. Sabir, Int. J. Hydrogen Energy 30 (2005) 359.
[4] X.D. Wang, Y.Y. Duan, W.M. Yan, J. Power Sources 173 (2007) 210.
[5] Y. Wang, C.Y. Wang, J. Power Sources 153 (2006) 130.
[6] L. Sun, P.H. Oosthuizen, K.B. McAuley, Int. J. Therm. Sci. 45 (2006) 1021.
[7] S.S. Hsieh, S.H. Yang, C.L. Feng, J. Power Sources 162 (2006) 262.
[8] J.P. Feser, A.K. Prasad, S.G. Advani, J. Power Sources 161 (2006) 404.
[9] X.D. Wang, Y.Y. Duan, W.M. Yan, J. Power Sources 172 (2007) 265.
[10] X.D. Wang, Y.Y. Duan, W.M. Yan, F.B. Weng, J. Power Sources 176 (2008) 247.
[11] X.D. Wang, Y.Y. Duan, W.M. Yan, X.F. Peng, J. Power Sources 175 (2008) 397.
[12] X.D. Wang, Y.Y. Duan, W.M. Yan, X.F. Peng, Electrochim. Acta 53 (2008) 5334.
[13] T.V. Nguyen, J. Electrochem. Soc. 143 (1996) L103.
[14] C. Xu, T.S. Zhao, Electrochem. Commun. 9 (2007) 497.
[15] S.W. Cha, R. O'Hayre, S.J. Lee, Y. Saito, F.B. Prinz, J. Electrochem. Soc. 151 (2004) 1856.
[16] M.V. Williams, H.R. Kunz, J.M. Fenton, J. Electrochem. Soc. 151 (2004) A1617.
[17] C. Xu, Y.L. He, T.S. Zhao, R. Chen, Q. Ye, J. Electrochem. Soc. 153 (2006) A1358.
[18] Q. Ye, T.S. Zhao, C. Xu, Electrochim. Acta 51 (2006) 5420.
[19] W.M. Yan, H.Y. Li, P.C. Chiu, X.D. Wang, J. Power Sources 178 (2008) 174.
[20] H.C. Liu, W.M. Yan, X.D. Wang, J. Electrochem. Soc. 154 (2007) B1338.
[21] F.B. Weng, A. Su, C.Y. Hsu, C.Y. Lee, J. Power Sources 157 (2006) 674.
[22] J. Scholta, F. Häussler, W. Zhang, L. Kuppers, L. Jörissen, W. Lehnert, J. Power Sources 155 (2006) 60.
[23] L. Wang, A. Husar, T.H. Zhou, H.T. Liu, Int. J. Hydrogen Energy 28 (2003) 1263.
[24] L. Wang, H.T. Liu, J. Power Sources 134 (2004) 185.
[25] T.V. Nguyen, M.W. Knobbe, J. Power Sources 114 (2003) 70.
[26] M. Amirinejad, S. Rowshanzamir, M.H. Eikani, J. Power Sources 161 (2006) 872.
[27] W.M. Yan, S.C. Mei, C.Y. Soong, Z.S. Liu, D. Song, J. Power Sources 160 (2006) 116.
[28] W.M. Yan, C.Y. Chen, S.C. Mei, C.Y. Soong, F. Chen, J. Power Sources 162 (2006) 1157.
[29] W.M. Yan, C.H. Yang, C.Y. Soong, F. Chen, S.C. Mei, J. Power Sources 160 (2006) 284.
[30] Q. Yan, H. Toghiani, H. Causey, J. Power Sources 161 (2006) 492.
[31] H. Xu, H.R. Kunz, J.M. Fenton, Electrochim. Acta 52 (2007) 3525.
[32] H. Sun, G.S. Zhang, L.J. Guo, D.H. Shang, H.T. Liu, J. Power Sources 168 (2007) 400.
[33] S.S. Hsieh, K.M. Chu, J. Power Sources 173 (2007) 222.
[34] J.L. Zhang, Y.H. Tang, C.J. Song, X. Cheng, J.J. Zhang, H.J. Wang, Electrochim. Acta 52 (2007) 5095.
[35] A.J.J. Kadjo, P. Brault, A. Caillard, C. Coutanceau, J.P. Garnier, S. Martemianov, J. Power Sources 172 (2007) 613.